Bio-Medical Materials and Engineering 24 (2014) 1895–1911
DOI 10.3233/BME-140999
IOS Press

Methods to quantitate videocapsule endoscopy images in celiac disease

Edward J. Ciaccio[a,*], Christina A. Tennyson[a], Govind Bhagat[a,b], Suzanne K. Lewis[a] and Peter H. Green[a]
[a]*Department of Medicine–Celiac Disease Center, Columbia University, New York, USA*
[b]*Department of Pathology and Cell Biology, Columbia University, New York, USA*

Abstract. In this work, bioengineering methods that can be used to quantitatively analyze videocapsule endoscopy images that have been acquired from celiac patients versus controls are described. For videocapsule endoscopic analysis, each patient swallows a capsule which contains an imaging device and light source. In celiac and control patients, images are acquired and analyzed at the level of the small intestine. The data used for videocapsule analysis consisted of high resolution images of dimension 576 × 576 pixels, acquired twice per second. The goal of the quantitative analysis is to detect abnormality in celiac patient images as compared with controls. Several types of abnormality can exist at the level of the small intestine in celiac patients. In untreated patients, and often even after treatment with a gluten-free diet, there can be villous atrophy, as well as presence of fissures and a mottled appearance. To detect and discern these abnormalities, several methods of statistical and structural feature extraction and selection are described. It was found that there is a significantly greater variation in image texture and average brightness level in celiac patients as compared with controls ($p < 0.05$). Celiac patients have a longer dominant period as compared with controls, averaging 6.4 ± 2.6 seconds versus 4.7 ± 1.6 seconds in controls ($p = 0.001$). This suggests that overall motility is slower in the celiac patients. Furthermore, the mean number of villous protrusions per image was found to be 402.2±15.0 in celiac patients versus 420.8±24.0 in control patients ($p < 0.001$). The average protrusion width was 14.66±1.04 pixels in celiacs versus 13.91±1.47 pixels in controls ($p = 0.01$). The mean protrusion height was 3.10±0.26 grayscale levels for celiacs versus 2.70±0.43 grayscale levels for controls ($p < 0.001$). Thus celiac patients tended to have fewer protrusions, and these were more varied in shape, tending to be blunted, as compared with controls, which more often had fine, uniform protrusions. A variety of computerized methods are now available to quantitate videocapsule images for comparison of celiac versus control patients. Since these methods are based on computer algorithms, they can be automated and there is no variation in the results due to observer bias. These methods readily lend themselves to automation, so that it may be possible to map the entire small intestine for presence of abnormality in real-time. It is also possible to develop an automated, quantitative clinical score which can be displayed with real-time update during the procedure. This would be useful to determine progress in celiac patients on a gluten-free diet, and to better understand the properties of the healing process in these patients.

Keywords: Celiac disease, endoscopy, imaging, small intestine, videocapsule

*Corresponding author: Edward J. Ciaccio, Department of Medicine–Celiac Disease Center, Columbia University, New York, USA. Tel.: 212 305 5447; Fax: 212 342 0447; Email: ciaccio@columbia.edu.

1. Introduction

Celiac disease is an autoimmune disease that can primarily affect the small intestinal mucosa, but may also have systemic effects on many organ systems including the heart and nervous system [1]. It is common but underdiagnosed [2], affecting about 1% worldwide, though relatively few are diagnosed even in the United States [3]. This is in part due to the lack of physician education and also the complexity in diagnosing the disease. Based on a positive antibody test, a patient may be suspected of having celiac disease. But for definitive diagnosis, endoscopy with intestinal biopsy should be used to determine if there is villous atrophy and other abnormalities in the small intestinal mucosa [1–3]. Celiac patient symptoms often resolve on a gluten-free diet, as the autoimmune response is directed toward the gluten protein [4]. This protein is found in wheat, rye, and barley. Thus celiac patients must eliminate these grains from their diet. However, not all celiac patients respond to the gluten-free diet. Some patients are refractory, meaning that there is little or no change in symptoms or small intestinal pathology despite the gluten-free diet [5]. Even in those patients who do partially resolve, there is often incomplete resolution of symptoms after being on the diet for many months or years [6].

The gold standard in the diagnosis of celiac disease is the presence of villous atrophy in biopsies of the duodenum. Part of the difficulty in diagnosing celiac disease is that the presence of villous atrophy in the small intestine can be missed using the standard endoscopic technique [7]. In celiac disease, villous atrophy is often subtle and patchy. Furthermore, the standard endoscope cannot extend throughout the small intestine to all regions where villous atrophy can occur. The degree of villous atrophy is graded microscopically using the Marsh score which ranges from I to IIIa, b, and c [8]. Patients with a Marsh score of III have villi that are atrophic. Furthermore, there are often abnormalities of the small intestinal mucosa visualized through the endoscope, such as the presence of fissuring and a mottled appearance reflecting the damage seen under the microscope. In Marsh I–II patients however, there may be no readily detectable alterations to the structural appearance of the intestine. If a quantitative, automated method to detect the presence of small intestinal abnormality could be developed, it would potentially be useful to diagnose celiac patients with lesser degrees of mucosal damage, via endoscopic imaging. It could also be useful to determine the exact degree of abnormality without user bias.

At the present time, satisfactory images of the small intestine can be obtained using a standard endoscope because the gastroenterologist can direct the camera lens so that it is perpendicular to the mucosal surface, and so that sufficient light from the endoscope illuminates the imaged area. Videocapsule endoscopy is a newer technique in which the camera is contained within a capsule that is swallowed by the patient [9,10]. High-resolution images are then acquired at a frequency of 2 per second. However, unlike the manual guidance for imaging that can be done using a standard endoscope, it is not currently possible to manually direct the videocapsule during the imaging process [11]. The capsule tumbles, and the images that result may be of low quality due to oblique camera-to-small intestinal mucosa angle, poor lighting, and/or incorrect distancing between camera and the area being imaged. Furthermore, presence of opaque intestinal fluids may obscure the mucosa during imaging. Thus only a fraction of videocapsule images are typically of excellent quality for detection of villous atrophy and other abnormalities in the small intestinal mucosa. This presents a significant problem for the use of the technique as a screening tool. However, the videocapsule method also has potentially significant advantages, including the ability to image the entire small intestine, and the lesser degree of invasiveness in use of the capsule, as compared with the standard endoscopic method.

In this review, we discuss the main methods that have been developed to quantitatively analyze the degree of abnormality in the small intestinal mucosa of celiac patients. We will mainly discuss videocapsule analysis, since this method would most benefit from a quantitative, automated technique to analyze the many thousands of small intestinal images that are acquired from each patient. Ideally, any such method should be able to rapidly analyze a set of retrospective small intestinal images from a particular patient, in a time period on the order of seconds or less. It would also be useful if the methodology could be adapted to real-time analysis, that is, for computer processing and detection and localization of abnormality within the period for image update, which is 0.5 seconds for currently available videocapsule imaging systems. Moreover, it would be quite helpful if the methodology could be utilized to develop a quantitative clinical score. Any such score would be free from dependency on user bias, and would provide a real number based on quantitative measurement. Herein we summarize our findings.

2. Materials and methods

2.1. Clinical procedure and data acquisition

Retrospective videocapsule endoscopy images were obtained from patients with celiac disease and from control patients [12]. In all except one patient, six biopsy specimens were obtained during endoscopy and then analyzed using light microscopy in accordance with guidelines [13]. In one celiac disease patient who also had hemophilia, biopsies were not obtained. The celiac patients who were biopsied were found to have Marsh grade II-IIIC lesions in the small intestinal mucosa, and positive serology for celiac disease.

Informed consent was obtained for each videocapsule endoscopy study. The exclusion criteria were: age under 18 years, history of or suspected small bowel obstruction, dysphagia, presence of electromedical implants, previous gastrointestinal surgery, pregnancy, or nonsteroidal anti-inflammatory drug (NSAID) use during the previous month. For analysis, only complete videocapsule endoscopy studies, reaching the colon, were used. The study was approved by the Institutional Review Board at Columbia University Medical Center.

The PillCam videocapsule (ver. SB2, 2007, Given Imaging, Yoqneam, Israel) [14] was used for acquiring images. The device includes a capsule, recorder unit, battery pack, wireless interface, and real-time viewer. The capsule is a single-use devise and acquires digital image frames at a 2/second rate, with a resolution of 576 × 576 pixels [14]. The capsule is 26 × 11 millimeters in size. For each patient undergoing the procedure, abdominal leads were positioned, and a belt containing the data recorder was placed at waist level. All subjects swallowed the videocapsule with radio transmitter in the early morning with approximately 200 milliliters of water and 80 milligrams of simethicone after an overnight fast without bowel preparation. Subjects were allowed to drink water two hours after capsule ingestion, and to eat a light meal four hours after capsule ingestion. The recorder was then removed, and the data downloaded to a HIPAA-compliant PC-based computer console equipped with RAPID software (ver. 5, 2008, Given Imaging, Yoqneam, Israel). The RAPID software was used for review and clinical report generation during the videocapsule endoscopy studies. Videos were interpreted by three experienced gastroenterologists.

Selected de-identified videoclips, 200 image frames in length (100 seconds of data), were exported to external media without patient identifiers for quantitative analysis. Images were acquired immediately distal to the pylorus, corresponding to the proximal duodenum (location 1). The

videocapsule endoscopic images of celiac patients that were used for analysis were taken from regions that appeared abnormal. All image sequences used for analysis were selected to have minimal presence of extraneous substances such as air bubbles and opaque fluids. From the portions of each videoclip meeting these criteria at each small intestinal level, the 200 image sequence used for analysis was randomly extracted. The total small bowel transit time of the videocapsule was divided into tertiles. Videoclips were also acquired from each of the three tertiles for each patient (locations 2, 3, and 4, roughly corresponding to the distal duodenum, the jejunum, and the proximal ileum, respectively). The actual image resolution depended on the camera–lumen distance.

2.2. Data preprocessing

The color videoclip was converted to a series of grayscale images for quantitative analysis. Thus 256 grayscale brightness levels, ranging from 0 = black to 255 = white, were extracted using Matlab Ver. 7.7, 2008 (The MathWorks, Natick MA). The image data were ported to software created by the authors, which was coded using the Intel Visual Fortran Compiler (ver. 9.0, 2005, Intel Corporation, Santa Clara CA).

2.3. Quantitative methods

Several quantitative methods were developed to analyze the videocapsule endoscopy images [12]. The idea was to construct features, which can be statistical or structural, to detect and describe the presence of abnormality in images of the small intestinal mucosa, and to distinguish said areas from normal areas of the small intestine.

2.3.1. Texture analysis

Texture analysis can be applied to analyze videocapsule images based on the pixel grayscale level. The simplest measure of variability is the standard deviation in pixel grayscale level. If the standard deviation in grayscale level is calculated over the entire image, presence of abnormality in a small portion of the image may be masked by the large portion of the image with normal mucosal properties, and normal image appearance. Therefore, for further clarity, each 576 × 576 videocapsule image was subdivided into 10 × 10 pixel subimage areas, excluding the edges [15]. The mean and standard deviation was calculated for each of these subimages. Then the mean or average grayscale level (termed the image brightness) and the standard deviation in grayscale level (termed the image texture) of each subimage was averaged for all subimages.

The process is in part illustrated in Figure 1. In panel A is an image acquired from a celiac patient videoclip of the distal duodenum after preprocessing the original color image to grayscale levels. The overall dimension of the image is 576 × 576 pixels. Examples of 10 × 10 pixel subimages are noted by black open squares. Close-up of the bolded subimage area is shown to the left. In panel B, the close-up is shown untouched. The actual 10 × 10 subimage is contained within the area bounded by the square. In panel C, the same close-up is shown but with contrast enhancement. The 10 × 10 subimage area is still shown bounded by the square. Note that substantial detail has become evident at the pixel level by using contrast enhancement. Based on the large amount of variation, this particular subimage would be expected to have a large texture as measured by the standard deviation in brightness level.

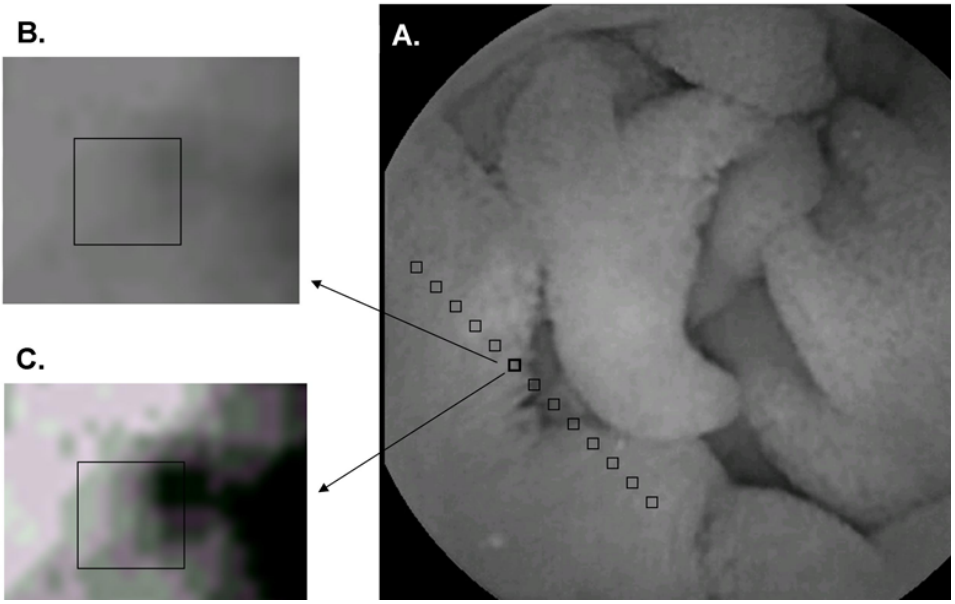

Fig. 1. Depiction of grayscale level videocapsule endoscopy image and various subimages, one of which is shown as a close-up.

The texture analysis statistical preprocessing technique can therefore assist in highlighting abnormal areas, as it would be expected that there would be a larger standard deviation in the brightness and texture overall, since the parameter values can vary from one subimage to the next where there is abnormality rather than uniformity. The mean values over 200 frames (100 seconds) of image sequence were used for analysis. Since presence of patchy villous atrophy, as well as presence of fissuring and mottled appearance, results in a spatially changing grayscale level and pattern, it would be expected that the abnormal features would be evident in the statistics of the brightness and in the variability features. Whereas, control images would be expected to have relatively uniform appearance, thus little or no spatial or temporal variability.

2.3.2. Texture subbands

Although image brightness and variability measurements are useful to obtain overall quantitative characteristics of each patient videoclip, to provide additional fine detail, textural features can be divided into subbands [16]. These measurements are done by graphing the brightness and texture of the subimages, for the entire 200 image videoclip sequence, using a scatterplot. The texture is plotted on the ordinate axis while the brightness is plotted on the abscissa. The total number of subimages in one videoclip sequence is $57 \times 57 \times 200 = 649{,}800$. Since the individual points would be visually obscured in a scatterplot, a select number, approximately 10% of the total, are actually plotted. The scatterplot is then divided into subbands according to texture, which is plotted on the ordinate axis. The 1st subband is defined as including those subimages having a texture of 0-10 (units are pixel brightness level). The average texture and the average brightness within this subband, and the actual

number of subimage values graphed in the subband, are used as measurement values. This is repeated for the 2nd subband (texture of 10-20 as measured by the standard deviation in pixel brightness) and the 3rd subband (texture of 20-30 as measured by the standard deviation in pixel brightness). Thus there are nine possible subband measurements. The use of texture subbands can be helpful to quantitate videocapsule images because the characteristics of texture and brightness in each of three subbands are considered separately, rather than lumping all measurements into a single band.

2.3.3. Motility estimation

Videocapsules can tumble as they move through the gastrointestinal system. The frame of reference can thus be moving as a capsule proceeds through the small intestine. As a first approximation, the progression of the videocapsule is related to gastrointestinal motility. However, to capture this relationship necessitates the presence of a fiducial mark within each image that can be used to gauge reference orientation. We selected the darkest 10,000 pixels per image to approximate the direction of the long axis of the small intestinal lumen [17]. Variation in the centroid of this dark region (i.e., variation in the mean dark pixel location along the x- and y-axes), and variation in the maximum width of the dark region (x-axis), were used as estimates of gastrointestinal motility and variation in the luminal diameter as caused in part by motility.

2.3.4. Shape-from-shading

Although each image is two-dimensional, it can be projected onto three dimensions using shape-from-shading principles [18]. The third dimension is formed according to the grayscale level of each pixel. The value along the third dimension is increased as pixel brightness increases. Darker pixels and darker image regions will be at greatest depth along the Z-axis, while brighter pixels and image regions will be present at shallower depth. Thus three-dimensional structure is formed from two-dimensional location plus pixel brightness level. Based on the three-dimensional structure, a syntax was developed to detect and measure luminal wall protrusions. Protrusions were defined as three-dimensional structural convexities having length, width, and height dimensions above preselected threshold values. If a particularly convexity lacked sufficient length, width, and/or height, it was not selected as a protrusion. The protrusions per image were counted, and their mean dimensions per image were determined, with the values being used for videocapsule quantitation.

2.3.5. Basis image transformation

A basis is a set of signals or images that can be used to construct a complex signal or image, respectively, from fundamental components. Videocapsule images are complex in terms of the varying detail, feature set, texture, and brightness level across the spatial entirety of the image, and from one image in the sequence to the next. It can be helpful to reduce complexity by describing an image series using basis images, which contain salient and fundamental components present in the videoclip sequence [19]. Analysis of basis images rather than the original images makes the measurements more robust to random extraneous features that are not a part of the actual luminal surface. The transformation can be helpful to retain repetitive components in the image sequence, while removing noise and extraneous substances such as air bubbles and opaque fluids [19]. Using a data-driven basis, the basis images themselves provide information concerning the complexities in the image series, as it is reduced to fundamental components. Moreover, by determining the weighting of each basis vector

that could be used to reconstruct each original image, detail concerning changes in image complexity from one image to the next can be obtained. Thus this method is also potentially useful for videocapsule quantitation.

2.3.6. Frequency analysis

Periodicities in the sequences of videocapsule images can occur, and these can be measured with proper quantitative technique [20]. One way to do this is to determine the mean image brightness of each of the 200 image frames of a videoclip sequence. This mean value can be considered to be a signal with a sampling interval of 0.5 seconds. It can be transformed into the frequency domain, and characteristics of the frequency content can then be calculated. An important component of the frequency spectrum is the dominant frequency (DF), which is defined as the frequency of the largest fundamental spectral peak (not a harmonic). Because the frequencies of this data are quite low [20], the values can be written as the Dominant Period (DP) which is simply 1/DF. It is likely that the frequency content of the image frames measured in this way is somewhat related to the motility of the small intestine at the level being imaged by the capsule [20]. When gastrointestinal motility is diminished, it would be hypothesized to result in a lower DF value over the sequence of 200 images. There is some evidence that celiac patients, particularly when untreated, have lesser gastrointestinal motility [21]. Thus the mean value of the DF, or DP, may be useful to compare celiacs versus controls and to detect areas of abnormality in celiac patients, in whom motility may be diminished.

3. Results

3.1. Imaging

Examples of an image sequence from a control patient videoclip is provided in Figure 2. These images were obtained from the same 200 image videoclip, at the level of the duodenum, and are unretouched. They were acquired up to a few seconds apart, with the time given at upper left. Although there are quite a few folds and changes in dimension and diameter, overall the images have similar appearance in terms of texture, color, and folding, both within each image, and from one image to the next. The texture appears similar throughout in terms of the fine detail as well as the characteristic shape and pattern. The direction of the long-axis of the lumen changes to some extent from one image to the next. The lighting appears to be approximately uniform except that regions along the long-axis of the lumen are at significantly greater depth from the camera and light source, and are therefore substantially darker in some images. These images are typical of those acquired from control patients at this anatomical level.

From the celiac patient videoclip, for which a portion of the sequence is displayed in Figure 2, basis images were constructed from the grayscale level values, examples of which are provided in Figure 3. The bases are numbered in order of importance from 1 through 8, with importance measured by the power in the image. All of the basis images are different, but they have similar level of detail, and similar shading and contrast level. As they were all generated from the videoclip image sequence

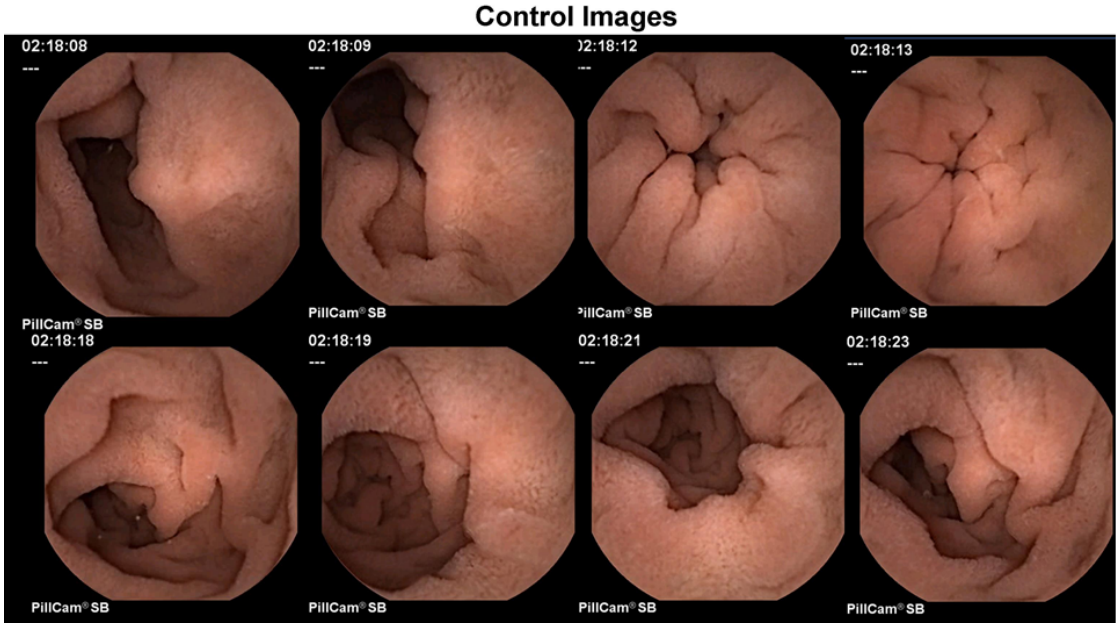

Fig. 2. Series of color videocapsule images obtained from a videoclip of a control patient at the level of the proximal duodenum. Time of each image capture is given.

partially shown in Figure 2, they represent the salient grayscale level features of this sequence. In combination with appropriate weighting, they could be used to reconstruct the grayscale version of any of the images shown in Figure 2, up to the 8th level of reconstruction detail. For the bases of Figure 3, the first is the most important. The first three basis images tend to have a darker region at center, which likely represents the long-axis direction of the lumen, where image areas are darker in Figure 2. Note that there are a number of faint black lines in many of the bases of Figure 3. These likely represent some of the luminal folds and their edges that are evident in the images of Figure 2.

In Figure 4 are shown examples of color images from a celiac patient videoclip sequence at about the level of the duodenal bulb. Note the deeper texture as compared with the control patient color images of Figure 2. The celiac patient surface includes both a varied texture and large changes in folding. Rather than uniformity as in Figure 2, Figure 4 gives the impression of heterogeneity both on the level of the spatial content of a single image, as well as in alterations of the content and characteristics of the lumen from one image to the next. The long axis of the lumen is not always evident in the celiac patient images of Figure 4, as though the luminal folds were more haphazard and less clearly demarcated along the small intestinal passageway. It is also evident that the folds have greatly varying thickness, and in some areas folding appears to be absent. There is a mottled appearance in some images of Figure 4 such as at center-right in the lower set of images. There are also likely to be actual fissures in the local-level detail, for example as interspersed with the mottled region, noted by * in a few images.

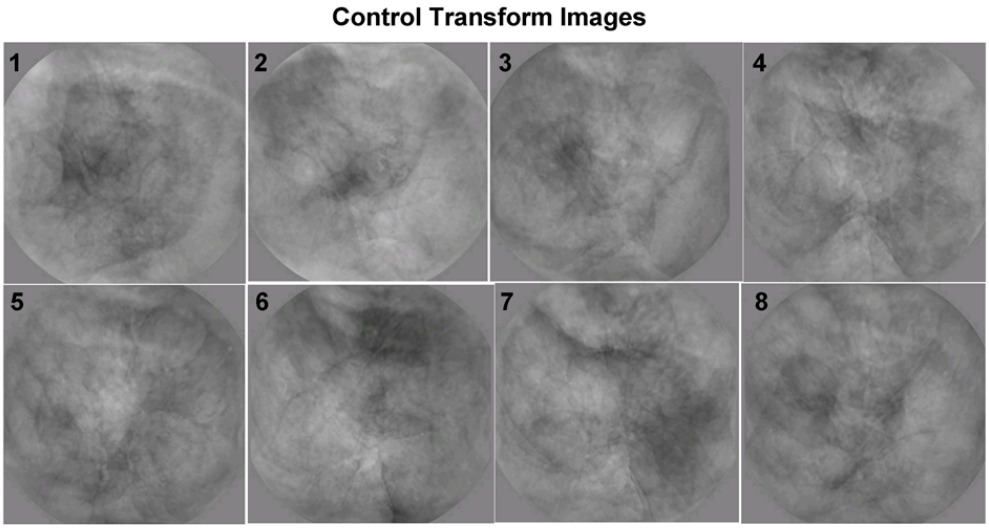

Fig. 3. The first eight transform basis images obtained from the same videoclip as is depicted in Fig. 2, after processing to grayscale level.

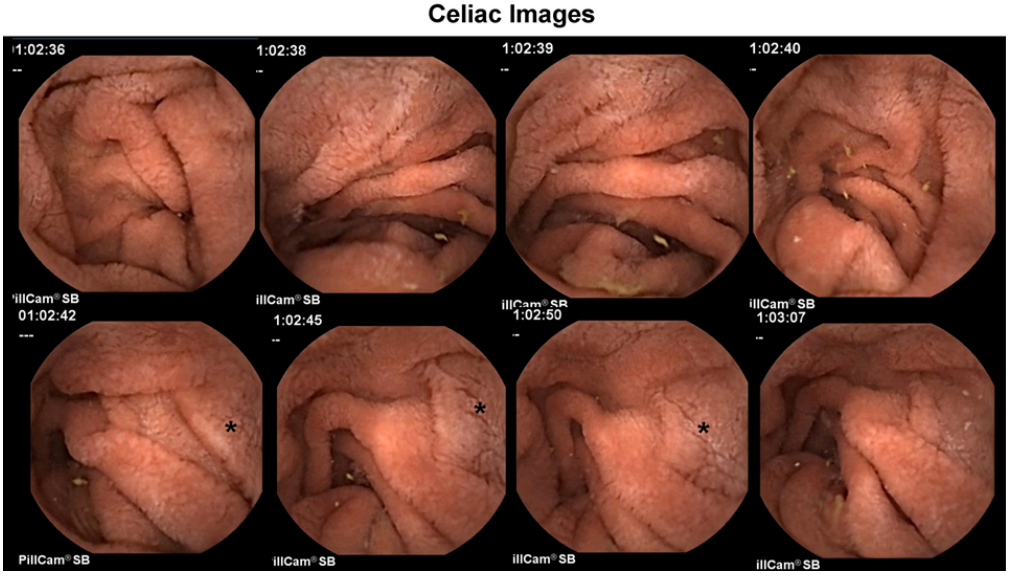

Fig. 4. Series of celiac color images from a videoclip at the level of the distal duodenum. The time in the sequence is given at upper left.

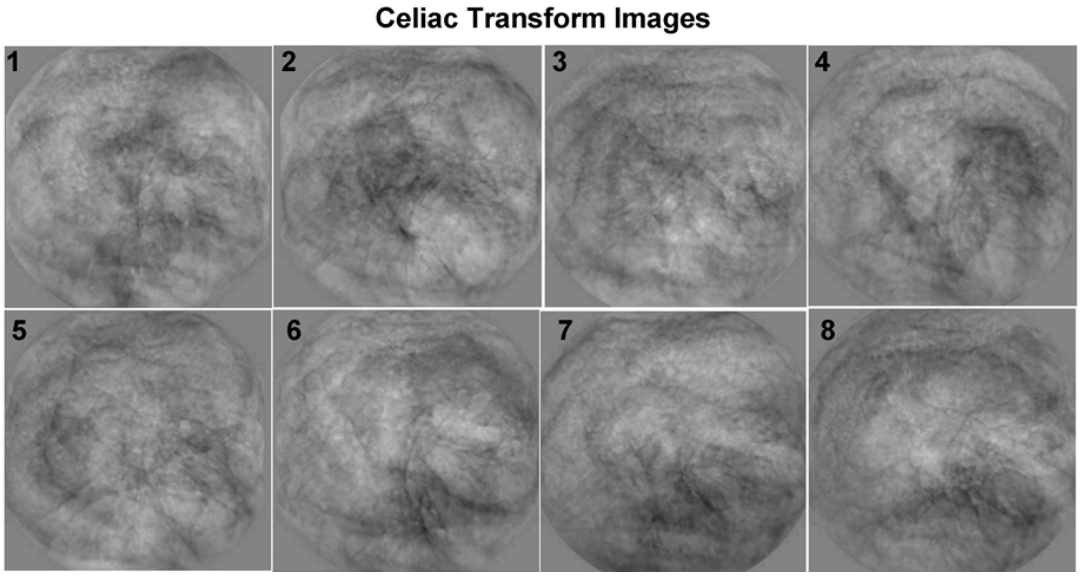

Fig. 5. The first eight transform basis images for the videoclip series depicted in Fig. 4. Note the large degree of detail and sharp changes in contrast in the basis images, which contain salient information common to the entire series of basis images of Fig. 4.

The first eight basis images for the celiac patient videoclip of Figure 4 are shown in Figure 5. There is substantial contrast and detail in these basis images as compared to the control patient bases of Figure 3. There are sharp changes in contrast and distinctive dark areas. There are areas that appear to be mottled and other areas where fissuring appears to be prevalent. These basis features directly result from the transformation of salient information that is evident in the original celiac videoclip, some of which is shown in Figure 4. The complexity in the luminal folding in Figure 4 is represented in the basis images of Figure 5 by the richness of the pattern variation, the large-scale alterations in texture across each individual basis image and from one basis image to the next, as well as by relatively sharp lines which in part represent edges of luminal folds. It is apparent from the evident differences in the features and characteristics of the celiac basis images (Figure 5) versus control basis images (Figure 3) that quantitative measurement of basis image texture may readily show differences for celiacs versus controls.

Besides texture measurements as determined from original and basis images, three-dimensional relationships can potentially be highly important for quantification of abnormality in videocapsule endoscopy images. An example for a control patient is depicted in Figure 6. At top left, panel A, is a single videoclip image acquired from the distal duodenum in a control patient after rendering into grayscale levels. The image is 576 × 576 pixels in dimension. When pixel brightness is converted into a third dimension, based on shape-from-shading principles [18], the result is shown in Figure 6B in false color. Pixel brightness level has been converted to depth, with darker pixels being deeper in the three-dimensional image of Figure 6B. Corresponding anatomical locations are noted by * as a reference in panels A and B. In panel B, it is evident that there are a number of protrusions on the

surface of the small intestinal lumen that appear to be fairly similar in density across the image, as well as in terms of their length, width, and height dimensions. In Figure 6C the presence of protrusions from panel B are noted by discs. Disc color denotes the value of the measured width of the protrusions of panel B. Smaller protrusions in terms of width, which is equal to the square root of the protrusion surface area, are noted by dark blue, while protrusions with larger width are noted by yellow, orange, and red color. These protrusions with larger width, and therefore larger surface area (= width^2), are few in this control patient videoclip series, and tend to be concentrated near the center of the image and at top. The number of pixels per width bin is shown in panel D. Most protrusions have a small width, with a sharp drop-off in the number of protrusions having larger widths.

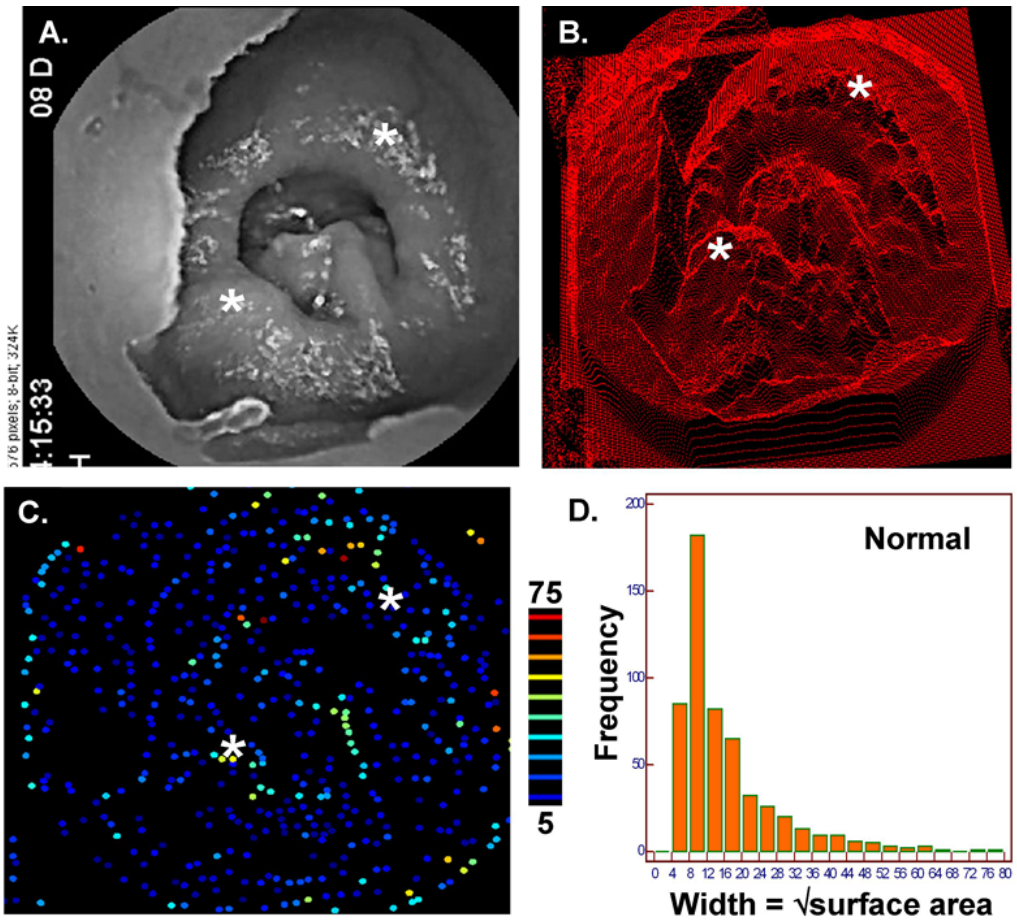

Fig. 6. A projection from two-dimensional image to three-dimensional structure using control patient data. A. grayscale patient two-dimensional image. B. three-dimensional structure. C. Location of projections in the three-dimensional structure. D. Histogram showing distribution of projections based on width. Most of the projections are narrow.

An example of the three-dimensional representation of a two-dimensional celiac patient image is shown in Figure 7. The two-dimensional image is depicted in panel A, and its three-dimensional representation based on shape-from-shading principles[18] is depicted in panel B. Two anatomical landmarks are noted by * for reference. The protrusion width map is shown in panel C. As in Figure 6, protrusions are noted by colored discs. However to better show detail, the color scale is inverted as compared with Figure 6C. Protrusions with lesser width, and therefore lesser surface area, are colored red, while those with greater surface area are colored blue. The histogram of protrusion width = √(surface area) is graphed in Figure 7D. As compared with the control patient (Figures 6C and 6D), the celiac patient protrusions have a greater variety of width values (Figures 7C and 7D). In other words, there is a greater variation in protrusion dimension. Furthermore, there is a tendency for protrusions to have a greater width, and therefore greater surface area. Thus as compared with the small intestinal mucosal structure of a control patient, which tends to be finely and uniformly textured, the celiac patient mucosal structure is more variable in texture in terms of a greater degree of clumpiness, and more varied protrusions extending from the luminal surface.

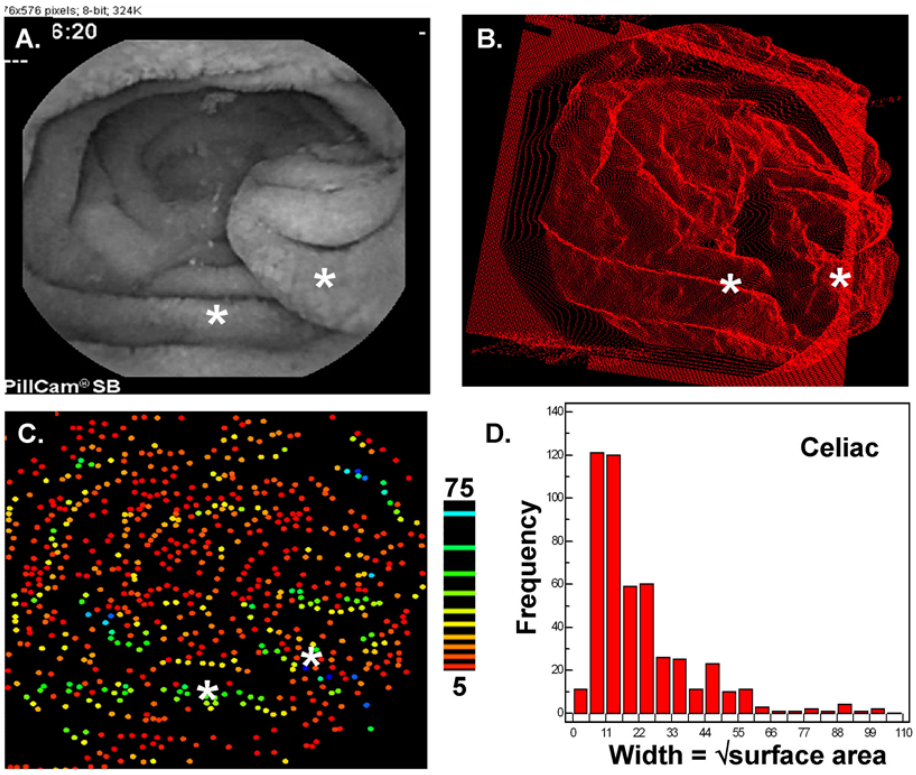

Fig. 7. A projection from two-dimensional image to three-dimensional structure using celiac patient data. A. grayscale patient two-dimensional image. B. three-dimensional structure. C. Location of projections in the three-dimensional structure. D. Histogram showing distribution of projections based on width. There is a range in widths of the projection, with some being relatively wide.

3.2. Summary statistics

Based on a number of previously published studies, the techniques outlined in the Methods section have been found useful to distinguish celiac versus control patients by videocapsule quantitation. Textural measurements, described in the Methods, potentially add greatly to the quantitation of videocapsule endoscopic imaging. It has been found previously, using 10 × 10 subimages for measurement over 200 image series, that the variability in image texture, which is derived from the standard deviation, is 0.43±0.47 grayscale brightness levels in celiac patients versus 0.29±0.25 grayscale brightness levels in control patients ($p<0.05$) [19]. Additionally it was found that variability in image brightness, which is derived from the mean, was 4.79 ± 2.43 grayscale brightness levels in celiacs versus 4.05 ± 1.72 grayscale brightness levels in controls ($p < 0.05$) [19]. Thus celiac images tend to have significantly greater variability in texture and brightness over 10 × 10 subimage areas as compared with control patient images. This may indicate the presence of more abnormal features in celiacs which may result from blunted and clumped villous architecture, fissuring, and mottled appearance of the small intestinal mucosa.

Using subbands, textural properties of videocapsule endoscopy images have also been used to distinguish celiac from control images at the level of the small intestine, with a sensitivity and specificity greater than 80% found using a test set [16]. Regarding the three-dimensional architecture, recently it has been determined that the mean number of villous protrusions per image is 402.2±15.0 in celiac patients versus 420.8±24.0 in control patients ($p < 0.001$) [18]. Moreover, average protrusion width was found to be 14.66±1.04 pixels in celiacs versus 13.91±1.47 pixels in controls ($p = 0.01$) [18]. The mean protrusion height was 3.10±0.26 grayscale levels for celiacs versus 2.70±0.43 grayscale levels for controls ($p < 0.001$) [18]. Thus celiac patients had significantly fewer protrusions on the luminal surface of the small intestine as compared with controls, and these protrusions had greater dimensions, suggesting they are indicative of a mosaic (cobblestone) macro-architectural pattern, which is commonly observed in celiac patient endoscopic images of the small intestine. Areas of mosaic pattern may indicate injury, which can possibly lead to changes in motility. In another study it was found that the dominant period, or DP, averaged 6.4 ± 2.6 seconds in celiacs versus 4.7 ± 1.6 seconds in controls ($p = 0.001$) [15]. The longer DP and therefore lower DF in celiacs is therefore possibly attributable to a lesser motility at areas of injury and abnormality in these patients.

4. Discussion

In this section, some of the advantages of using quantitative methods for videocapsule endoscopy analysis will be discussed. These will be contrasted with the difficulties that can occur when manual clinical scoring of both videocapsule and standard endoscopic images is used for analysis.

4.1. Clinical correlates

Videocapsule endoscopy has a number of advantages over standard endoscopy which would make improved and automated quantitation of the capsule images all the more useful. For example, direct examination using a standard endoscope is only possible for a short proximal region of the small intestine [22]. By comparison, videocapsule imaging can be utilized throughout the small intestine to

capture fine details in the appearance of small bowel mucosa that may be characteristic of celiac disease, including loss of folds, nodularity, scalloping, and mosaic pattern [22]. Furthermore, for all types of endoscopy, prior endoscopic experience increases the ability to interpret capsule endoscopy more accurately [23], but interobserver bias may still exist. By comparison, automated quantitation of videocapsule endoscopy images introduces no observer bias; thus would not be subject to the amount of training in the detection of clinical features.

Most studies that have attempted to distinguish celiac patient endoscopic images with abnormality versus controls have been less quantitative and more based upon visual inspection. Videocapsule endoscopy can be used to detect subtle mucosal lesions that may not be readily apparent by standard endoscopy [24]. For depiction of subtle mucosal lesions, elsewhere it has been found that the sensitivity is 92.9% while the specificity is 80% [24]. A recent meta-analysis compiling data from six studies videocapsule endoscopy studies demonstrated an overall pooled sensitivity of 89% and specificity of 95% when using clinical features [25]. In another study, videocapsule endoscopy was show to provide sensitivity of 87.5% and specificity of 90.9% for the visual detection of villous atrophy in patients with suspected celiac disease [26]. Variations in clinical statistical results from one study to the next may occur in part depending on the level of experience in reading videocapsule endoscopy clips, which have been found to have a significant impact on diagnostic findings [27]. Interobserver agreement for the diagnosis of celiac disease by videocapsule endoscopy is also variable and can range from 79.2 and 94.4% [26]. Other investigators have shown similar levels of sensitivity and specificity for detecting scalloping, mosaic pattern, micronodularity, and reduction of folds, features common to celiac disease, with values of sensitivity ranging from 70–90.5% and specificity ranging from 63.6–100% [26–30]. By comparison, results using automated quantitation of videocapsule sequences, as described herein, compares favorably to the manual, clinically derived techniques, with sensitivity varying from 80 – 88% and specificity varying from 80–96% in a test set [16]. Similar good results for videocapsule endoscopy studies are possible both in younger as well as in elderly patients [31].

4.2. Future trends

Recently a number of new techniques have been applied to improve videocapsule endoscopy automated quantitation. Endoscopy image distortion is common for both standard endoscopy and videocapsule endoscopy, but it is very difficult to remedy. When endoscope distortion correction was used prior to computer-assisted celiac disease diagnosis, no evident improvement in classification ability was achieved [32]. It is also possible to use scale-invariant texture descriptors for classifying celiac disease [33]. However, scale invariance is not necessarily a key feature for the successful classification of celiac disease datasets. In recent work, a polling protocol has been implemented to make the quantitative process more robust to outliers [12]. A large 24 feature set was automatically calculated, and threshold levels were used to distinguish celiac versus nonceliac values of each feature set. The entire feature set was then polled, with the majority vote winning, and the possibility of a tie if there were 12 feature values each in the celiac and in the nonceliac vote columns. This method was found to be more robust to the possibility that a particular feature may not work well for all videocapsule image data.

4.3. Limitations

Although we have described a number of techniques for videocapsule endoscopy quantitation, the discussion was meant to be a survey and not an exhaustive documentation of all techniques that have been proposed and implemented. Although 200 image videoclips were suggested as a standard sequence length for analysis of celiac versus control data at one of four anatomical regions of the small intestine, other sequence lengths, and other anatomic levels for analysis, may work just as well or possibly even better, the subject of future study. Many, though not all, videocapsule quantitation studies convert the original color image sequence to grayscale level for simplicity. Application of color images for analysis could improve findings, since color information may provide helpful additional detail for quantitation.

5. Conclusion

Progress is being made in the quantitation of videocapsule endoscopy images. Previously, only clinical scoring had been available, which can be biased and is mostly a qualitative method to assess images for presence of abnormality. Using quantitative techniques, it is possible to provide a real number score, which is unbiased and can be automated. Textural analysis, frequency analysis, projection of images to three dimensions, and the use of markers of motility are some of the recent focus areas for image quantitation.

Acknowledgement

The implementation of this study was made possible in part with a grant from the Celiac Sprue Association Peer Review Research Grant Program.

References

[1] P.H. Green, The many faces of celiac disease: Clinical presentation of celiac disease in the adult population, Gastroenterology **128** (2005), S74–S78.
[2] P.H.R. Green and C. Cellier, Celiac disease, N. Engl. J. Med. **357** (2007), 1731–1743.
[3] P.H.R. Green and B. Jabri, Coeliac disease, The Lancet **362** (2003), 383–391.
[4] K. Mustalahti, S. Lohiniemi, P. Collin, N. Vuolteenaho, P. Laippala and M. Mäki, Gluten-free diet and quality of life in patients with screen-detected celiac disease, Eff. Clin. Pract. **5** (2002), 105–113.
[5] A. Rubio-Tapia and J.A. Murray, Classification and management of refractory coeliac disease, Gut **59** (2010), 547–557.
[6] D.H. Dewar, S.C. Donnelly, S.D. McLaughlin, M.W. Johnson, H.J. Ellis and P.J. Ciclitira, Celiac disease: Management of persistent symptoms in patients on a gluten-free diet, World J. Gastroenterol. **18** (2012), 1348–1356.
[7] A.D. Hopper, R. Sidhu, D.P. Hurlstone, M.E. McAlindon and D.S. Sanders, Capsule endoscopy: An alternative to duodenal biopsy for the recognition of villous atrophy in coeliac disease? Digestive and Liver Disease **39** (2007), 140–145.
[8] P.J. Wahab, J.W. Meijer and C.J. Mulder, Histologic follow-up of people with celiac disease on a gluten-free diet: Slow and incomplete recovery, Am. J. Clin. Pathol. **118** (2002), 459–463.
[9] P.H. Green and M. Rubin, Capsule endoscopy in celiac disease, Gastrointest. Endosc. **62** (2005), 797–799.

[10] P.H. Green and M. Rubin, Capsule endoscopy in celiac disease: Diagnosis and management, Gastrointest. Endosc. Clin. N. Am. **16** (2006), 307–316.
[11] A. Moglia, A. Menciassi, P. Dario and A. Cuschieri, Capsule endoscopy: Progress update and challenges ahead, Nat. Rev. Gastroenterol. Hepatol. **6** (2009), 353–362.
[12] E.J. Ciaccio, C.A. Tennyson, G. Bhagat, S.K. Lewis and P.H. Green, Implementation of a polling protocol for predicting celiac disease in videocapsule analysis, World J. Gastrointest. Endosc. **5** (2013), 313–322.
[13] S. Serra and P.A. Jani, An approach to duodenal biopsies, J. Clin. Pathol. **59** (2006), 1133–1150.
[14] Y.C. Metzger, S.N. Adler, A.B. Shitrit, B. Koslowsky and I. Bjarnason, Comparison of a new PillCam™ SB2 video capsule versus the standard PillCam™ SB for detection of small bowel disease, Reports in Medical Imaging **2** (2009), 7–11.
[15] E.J. Ciaccio, C.A. Tennyson, S.K. Lewis, S. Krishnareddy, G. Bhagat and P.H. Green, Distinguishing patients with celiac disease by quantitative analysis of videocapsule endoscopy images, Comput. Methods Programs Biomed. **100** (2010), 39–48.
[16] E.J. Ciaccio, C.A. Tennyson, G. Bhagat, S.K. Lewis and P.H. Green, Classification of videocapsule endoscopy image patterns: Comparative analysis between patients with celiac disease and normal individuals, BioMed. Eng. OnLine **9** (2010), 44.
[17] E.J. Ciaccio, C.A. Tennyson, G. Bhagat, S.K. Lewis and P.H. Green, Quantitative estimates of motility from videocapsule endoscopy are useful to discern celiac patients from controls, Dig. Dis. Sci. **57** (2012), 2936–2943.
[18] E.J. Ciaccio, C.A. Tennyson, G. Bhagat, S.K. Lewis and P.H. Green, Use of shape-from-shading to estimate three-dimensional architecture in the small intestinal lumen of celiac and control patients, Comput. Methods Programs Biomed. **111** (2013), 676–684.
[19] E.J. Ciaccio, C.A. Tennyson, G. Bhagat, S.K. Lewis and P.H. Green, Transformation of videocapsule images to detect small bowel mucosal differences in celiac versus control patients, Comput. Methods Programs Biomed. **108** (2012), 28–37.
[20] E.J. Ciaccio, C.A. Tennyson, G. Bhagat, S.K. Lewis and P.H. Green, Robust spectral analysis of videocapsule images acquired from celiac disease patients, BioMed. Eng. OnLine **10** (2011), 78.
[21] A. Tursi, Gastrointestinal motility disturbances in celiac disease, J. Clin. Gastroenterol. **38** (2004), 642–645.
[22] U. Kopylov and E.G. Seidman, Clinical applications of small bowel capsule endoscopy, Clin. Exp. Gastroenterol. **6** (2013), 129–137.
[23] R. Sidhu, P. Sakellariou, M.E. McAlindon, J.S. Leeds, K. Shafiq, B.S. Hoeroldt, A.D. Hopper, M. Karmo, C. Salmon, D. Elphick, A. Ali and D.S. Sanders, Is formal training necessary for capsule endoscopy? The largest gastroenterology trainee study with controls, Digestive and Liver Disease **40** (2008), 298–302.
[24] D.W. Crook, P.R. Knuesel, J.M. Froehlich, F. Eigenmann, M. Unterweger, H.-J. Beer and R.A. Kubik-Huch, Comparison of magnetic resonance enterography and video capsule endoscopy in evaluating small bowel disease, European Journal of Gastroenterology & Hepatology **21** (2009), 54–65.
[25] T. Rokkas and Y. Niv, The role of video capsule endoscopy in the diagnosis of celiac disease: a meta-analysis, Eur. J. Gastroenterol. Hepatol. **24** (2012), 303–308.
[26] E. Rondonotti, C. Spada, D. Cave, M. Pennazio, M.E. Riccioni, I. De Vitis, D. Schneider, T. Sprujevnik, F. Villa, J. Langelier, A. Arrigoni, G. Costamagna and R. de Franchis, Video capsule enteroscopy in the diagnosis of celiac disease: A multicenter study, Am. J. Gastroenterol. **102** (2007), 1624–1631.
[27] E. Rondonotti, J.M. Herrerias, M. Pennazio, A. Caunedo, M. Mascarenhas-Saraiva and R. de Franchis, Complications, limitations, and failures of capsule endoscopy: A review of 733 cases, Gastrointest. Endosc. **62** (2005), 712–716.
[28] R. Petroniene, E. Dubcenco, J.P. Baker, C.A. Ottaway, S.J. Tang, S.A. Zanati, C.J. Streutker, G.W. Gardiner, R.E. Warren and K.N. Jeejeebhoy, Given capsule endoscopy in celiac disease: Evaluation of diagnostic accuracy and interobserver agreement, Am. J. Gastroenterol. **100** (2005), 685–694.
[29] F. Biagi, E. Rondonotti, J. Campanella, F. Villa, P.I. Bianchi, C. Klersy, R. De Franchis and G.R. Corazza, Video capsule endoscopy and histology for small-bowel mucosa evaluation: A comparison performed by blinded observers, Clin. Gastroenterol. Hepatol. **4** (2006), 998–1003.
[30] A.D. Hopper, R. Sidhu, D.P. Hurlstone, M.E. McAlindon and D.S. Sanders, Capsule endoscopy: An alternative to duodenal biopsy for the recognition of villous atrophy in coeliac disease? Dig. Liver Dis. **39** (2007), 140–145.
[31] S. Giuseppe, F. Russo, M.R. Franco, P. Sarracco, L. Pietrini and I. Sorrentini, Age and video capsule endoscopy in obscure gastrointestinal bleeding: A prospective study on hospitalized patients, Digestive Diseases Sciences **56** (2011), 1188–1193.

[32] M. Gschwandtner, M. Liedlgruber, A. Uhl and A. Vécsei, Experimental study on the impact of endoscope distortion correction on computer-assisted celiac disease diagnosis, 10th IEEE International Conference on Information Technology and Applications in Biomedicine, 2010, 1–6.
[33] S. Hegenbart, A. Uhl, A. Vécsei and G. Wimmer, Scale invariant texture descriptors for classifying celiac disease, Med. Image Anal. **17** (2013), 458–474.